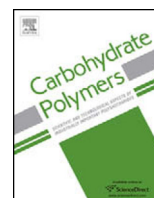




Since January 2020 Elsevier has created a COVID-19 resource centre with free information in English and Mandarin on the novel coronavirus COVID-19. The COVID-19 resource centre is hosted on Elsevier Connect, the company's public news and information website.

Elsevier hereby grants permission to make all its COVID-19-related research that is available on the COVID-19 resource centre - including this research content - immediately available in PubMed Central and other publicly funded repositories, such as the WHO COVID database with rights for unrestricted research re-use and analyses in any form or by any means with acknowledgement of the original source. These permissions are granted for free by Elsevier for as long as the COVID-19 resource centre remains active.



Nano zinc oxide–sodium alginate antibacterial cellulose fibres



Kokkarachedu Varaprasad^{a,*}, Gownolla Malegowd Raghavendra^b,
Tippabattini Jayaramudu^c, Jongchul Seo^b

^a Centro de Investigación de Polímeros Avanzados, CIPA, Beltrán Mathieu 224, piso 2, Concepción, Chile

^b Department of Packaging, Yonsei University, 1 Yonseidae-gil, Wonju, Gangwon-do 220-710, South Korea

^c Center for EAPap Actuator, Department of Mechanical Engineering, Inha University, 253 Yonghyun-Dong, Nam-Ku, Incheon 402-751, South Korea

ARTICLE INFO

Article history:

Received 28 July 2015

Received in revised form 17 August 2015

Accepted 25 August 2015

Available online 28 August 2015

Keywords:

Nano zinc oxide

Sodium alginate

Cellulose fibres

Wurtzite structure

Antibacterial fibres

ABSTRACT

In the present study, antibacterial cellulose fibres were successfully fabricated by a simple and cost-effective procedure by utilizing nano zinc oxide. The possible nano zinc oxide was successfully synthesized by precipitation technique and then impregnated effectively over cellulose fibres through sodium alginate matrix. XRD analysis revealed the 'rod-like' shape alignment of zinc oxide with an interplanar d-spacing of 0.246 nm corresponding to the (1 0 1) planes of the hexagonal wurtzite structure. TEM analysis confirmed the nano dimension of the synthesized zinc oxide nanoparticles. The presence of nano zinc oxide over cellulose fibres was evident from the SEM–EDS experiments. FTIR and TGA studies exhibited their effective bonding interaction. The tensile stress–strain curves data indicated the feasibility of the fabricated fibres for longer duration utility without any significant damage or breakage. The antibacterial studies against *Escherichia coli* revealed the excellent bacterial devastation property. Further, it was observed that when all the parameters remained constant, the variation of sodium alginate concentration showed impact in devastating the *E. coli*. In overall, the fabricated nano zinc oxide–sodium alginate cellulose fibres can be effectively utilized as antibacterial fibres for biomedical applications.

© 2015 Elsevier Ltd. All rights reserved.

1. Introduction

In the surgical zone, a lot of priorities has been given for protecting a surgical team from the patients' infectious blood and other bodily fluids. The spread of infections like HIV, hepatitis viruses, severe acute respiratory syndrome (SARS), etc., through contamination, has created increased pressure for the protection of the personnel with antimicrobial clothing. Therefore, surgical fabrics should necessarily possess antimicrobial properties (Ambika & Sundrarajan, 2015; Mucha, Hoter, & Swerev, 2002; Vaideki, Jayakumar, Rajendran, & Thilagavathi, 2008). The antimicrobial fabric when applied as wound dressings, it not only act as normal wound dressing but also provide hygienic atmosphere around the wound (Raghavendra, Varaprasad, & Jayaramudu, 2015). Generally, the fibre used in the wound dressing functional clothing contains cellulose, a homopolymer of β -D-glucopyranose units linked together by (1 \rightarrow 4)-glycosidic bonds (Raghavendra, Jayaramudu, Varaprasad, Sadiku, Ray, & Mohana Raju, 2013). The three-hydroxyl

groups in the cellulose acts as bonding sites for the external entities (Gardner, Oporto, Mills, & Samir, 2008).

In recent years, metal nanoparticles were extensively used as antibacterial agents towards many pathogens (Jayaramudu, Raghavendra, Varaprasad, Sadiku, & Raju, 2013; Jayaramudu, Raghavendra, Varaprasad, Sadiku, Ramam, et al., 2013; Raghavendra, Jayaramudu, Varaprasad, Mohan Reddy, & Raju, 2015). Among the various metal nanoparticles, silver nanoparticles were extensively studied because of their potential anti-bacterial properties (Kolya, Pal, Pandey, & Tripathy, 2015). However, the use of silver nanoparticles for medical applications is potentially limited due to their genotoxicity towards mammalian cell and their non-specific biological toxicity (Nagender Reddy, Eladia Maria, & Josef, 2009; Gardner et al., 2008). Alternatively, ZnO serves as an effective entity for devastating the microbial growth. Moreover, the raw material required for synthesis of ZnO is available at lower cost.

ZnO is an interesting transition metal oxide possess good catalytic, electrical, photochemical and optical properties; it is used in the area of bioscience as a biomimetic membrane; it can immobilize and modify proteins because of the fast electron transfer between the enzyme's active sites and the electrode (Gunalan, Sivaraj, & Rajendran, 2012). In addition, ZnO has several advantages: noticeable activity in the pH neutral region (pH = 7–8)

* Corresponding author.

E-mail addresses: varmaindian@gmail.com, prasad@cipachile.cl (K. Varaprasad).

without the presence of light (Trandafilović, Božanić, Dimitrijević-Branković, Luyt, & Djoković, 2012); it is non-toxic and chemically stable under exposure to both high temperatures and UV (Ambika & Sundrarajan, 2015).

Stabilization of the nanoparticles is an important factor that plays a key role for effective existence of the nanoparticles without aggregation. Natural polysaccharides are extensively used for this purpose. Sodium alginate is one such natural polysaccharide, chemically it is the sodium salt of alginic acid, an unbranched copolymer with homopolymeric blocks of β -1,4-linked-D mannuronic acid and α -1,4-linked-L-gulonic acid (Kolya et al., 2015; Varaprasad et al., 2015). Further, due to its good tissue compatibility, it has been widely used in the field of tissue engineering including regeneration of skin, cartilage, bone and liver and in the treatment of exuding wounds and in enhancing the healing process (Shalumon et al., 2011). Owing to the close relevance to the biomedical field, sodium alginate was particularly chosen for stabilization and binding of the synthesized nano ZnO over cellulose fibre.

Keeping all these perspectives in mind the present investigation was undertaken to fabricate antibacterial cellulose fibres from nano zinc oxide and sodium alginate for effective biomedical applications.

2. Materials

Zinc nitrate ($\text{Zn}(\text{NO}_3)_2$), sodium alginate (SA) and ammonium hydroxide (NH_4OH) were obtained from Sigma–Aldrich Chemicals Company and were used as received without further purification. Cellulose cotton fibres were purchased from SIMCO thread mills (Salem, Chennai, India). Double distilled water was used in all the experiments. All the reaction processes were carried out at room temperature, under ambient reaction conditions.

2.1. Preparation of nano zinc oxide–sodium alginate antibacterial cellulose fibres

2.1.1. Synthesis of zinc oxide nanoparticles (nano ZnO)

Zinc oxide nanoparticles (nano ZnO) was synthesized by a precipitation technique. In this technique, zinc nitrate (0.05 mol) was completely dissolved in 50 mL of distilled water in a 250 mL beaker under the constant stirring condition at room temperature for 1 h. To this aqueous solution, ammonium hydroxide was slowly added dropwise until a white colour precipitate was formed during which the pH was adjusted to 9. After stirring for 3 h, the precipitate was washed several times with distilled water till the pH of the filtrate was reduced to 7 and boiled for 5 min in order to obtain improved crystallization of the nano zinc oxide. The resultant precipitate was dried at 120 °C for 2 h.

2.1.2. Preparation of nano zinc oxide–sodium alginate cellulose fibres (ZnO–SACNF)

Initially, 0.5, 1.0 and 1.5% of aqueous sodium alginate solutions were prepared individually under constant stirring condition by dissolving the respective amount of sodium alginate in distilled water at room temperature for 4 h. To these solutions, nano zinc oxide (100 mg) was introduced and stirred at the constant stirring condition of 300 rpm for 1 h, then sonicated for 30 min to make the solutions homogeneous. To the prepared solutions, known amount of cellulose fibres were placed in an orbital shaking incubator at 300 rpm for 24 h at room temperature, and finally sonicated for 30 min. A rotation followed by sonication allows the nano zinc oxide to impregnate effectively over the cellulose fibres. Finally, the resulted nano zinc oxide–sodium alginate cellulose fibres (ZnO–SACNF) were taken out, dried at room temperature and utilized for further experimental characterization.

Based on the concentration of sodium alginate used for the fabrication of ZnO–SACNF fibres, the fibres were coded as ZnO–SACNF₁, ZnO–SACNF₂ and ZnO–SACNF₃ for 0.5%, 1% and 1.5% sodium alginate solutions, respectively.

Analogous to the above fabricated fibres (ZnO–SACNFs), a set of fibres from cellulose fibres and SA without nano ZnO were also fabricated. These fibres were named as sodium alginate coated cellulose fibres (SACFs) and used as reference samples.

3. Characterizations

Fourier transform infrared (FTIR) spectra of nano ZnO and ZnO–SACNF fibres were obtained from a Perkin Elmer, UATR two, FTIR spectrometer (Beaconsfield, Bucks, UK) in the wavelength range of 4000–500 cm^{-1} . Signal averages were obtained from 25 scans at a resolution of 1 cm^{-1} . SEM micrographs and Energy dispersive spectroscopy analyses for Zinc oxide were carried out using JEOL JEM 7500F SEM (Tokyo, Japan) scanning electron microscope at 2 keV. Microstructure and elemental observations of ZnO–SACNF fibres were carried out by scanning electron microscope energy dispersive spectroscopy (SEM–EDS, Philips XL 30) analyses. Transmission electron microscopes were recorded on JEM-1200EX, JEOL (Tokyo, Japan). The samples were dispersed in 1:1 methanol and water solution, and deposited on a 3 mm copper grid and dried at ambient temperature after removing the excess solution using filter paper. X-ray diffraction measurements were carried out using a Rigakudiffractometer with $\text{Cu-K}\alpha$ radiation and using a scan rate 0.02° s^{-1} . Thermal characteristics of zinc oxide the cellulose nanocomposite fibres were determined from the thermogravimetric analysis (TGA) data, using TGA Q 50 thermal analyzer (T.A. Instruments–Water LLC, Newcastle, DE, USA), at a heating rate of 10 °C/min and passing nitrogen gas at a flow rate of 100 mL/min. Tensile (tensile strength, modulus and % elongation-at-break) properties were determined by using INSTRON 3369 Universal Testing Machine (Buckinghamshire, England). The sample fibres were cut into 1 mm \times 100 mm and mechanical properties were studied using 10 kg load cell by maintaining a gauge length of 50 mm, by operating the machine at a crosshead speed of 5 mm/min and at 23 °C.

3.1. Antibacterial test

Antibacterial activity of the cellulose zinc nanocomposite fibres were tested against *Escherichia coli* by following the method adopted by us in our previous research works (Jayaramudu, Raghavendra, Varaprasad, Sadiku, & Raju, 2013; Raghavendra et al., 2013; Raghavendra, Varaprasad, & Jayaramudu, 2015). In brief, the required nutrient agar medium was prepared by mixing peptone (5.0 g), beef extract (3.0 g), sodium chloride (5.0 g) and agar (15.0 g) in 1000 mL of distilled water, and the pH was adjusted to 7.0. The agar medium was sterilized in a conical flask at a pressure of 15 lbs in^{-2} for 30 min and transferred into sterilized Petri dishes in a laminar air flow chamber (Microfilt Laminar Flow Ultra Clean Air Unit, Mumbai, India) for solidification. Later, 50 μL microbial culture was uniformly streaked over the solid surface. Into this inoculated Petri dish, the sample fibres were placed and incubated at 37 °C for 48 h to obtain inhibition zone. Finally, the formed inhibition zone were measured and photographed.

4. Results and discussion

Fabrication of nano zinc oxide cellulose fibres signifies one of the best antibacterial fibres for biomedical applications. During the typical process nano zinc oxide–sodium alginate cellulose fibres (ZnO–SACNF) were fabricated by effective impregnation of sodium

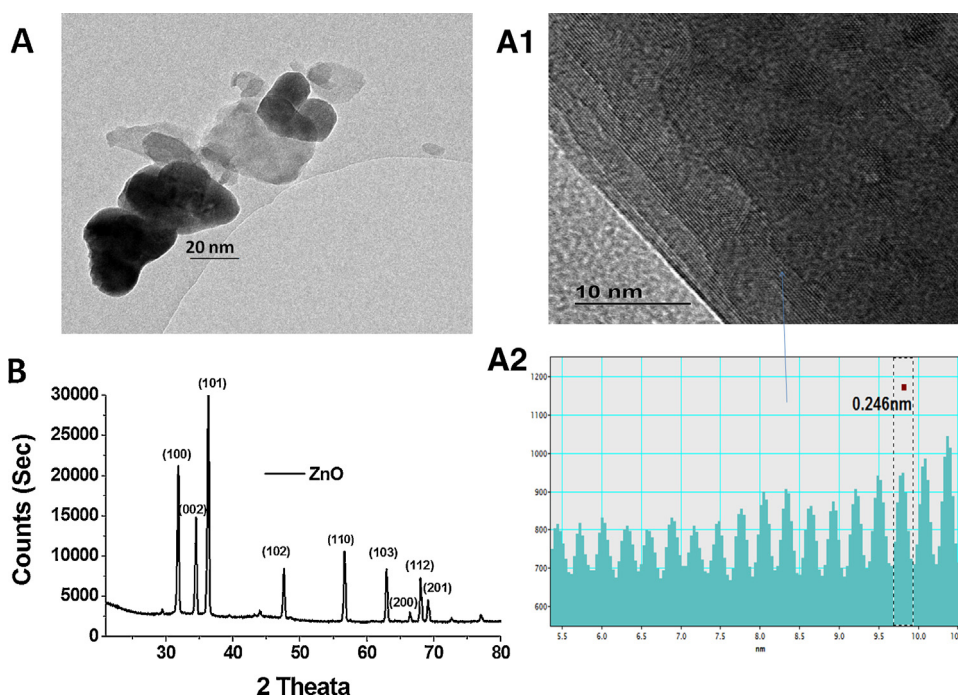
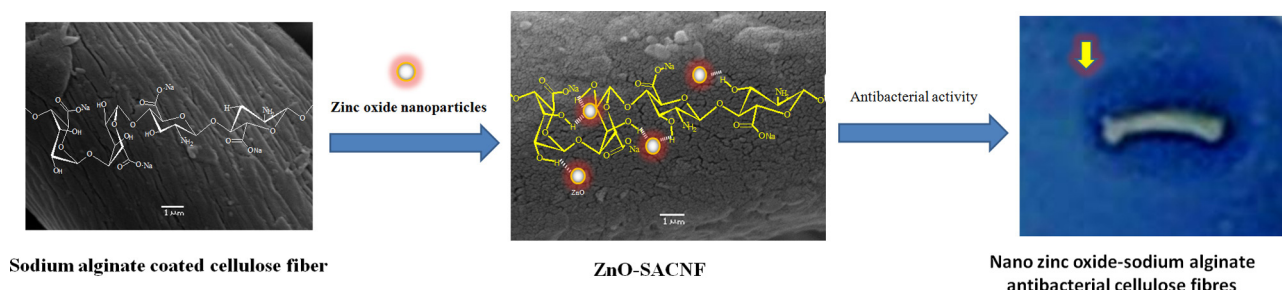
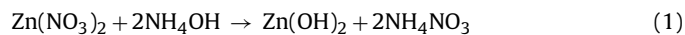


Fig. 1. (A) TEM image of Zinc oxide, (A1) higher resolution of zinc oxide TEM and (A2) inter-planar d-spacing image; (B) XRD pattern of nano zinc oxide.

alginate stabilized nano ZnO over cellulose fibres. The possible nano ZnO was synthesized by quantitatively utilizing the zinc nitrate and ammonium hydroxide. The possible reactions are shown in Eqs. (1) and (2). The development of ZnO-SACNF was schematically shown in Scheme 1.



The TEM image of typical nano zinc oxide is shown in Fig. 1A. It can be seen that the synthesized nano zinc oxide particles are in different shape and agglomerated possessing an average diameter of 25 ± 5 nm. At higher resolution, the inter-planar d-spacing of the lattice plane 0.246 nm is clearly visible in Fig. 1A2, corresponding to the (101) planes of wurtzite zinc oxide which is in agreement with previously reported values (Zhao et al., 2014). These studies clearly specify that the precipitation route supports the formation of the well-defined structure of zinc oxide material, which enhances their applicability in medical and advanced material science applications.

The XRD pattern of nano zinc oxide is shown in Fig. 1B. The XRD pattern shows well-intensified peaks for the developed zinc oxide nanoparticles. The pattern of pure zinc oxide shows the diffraction peaks of crystalline zinc oxide corresponding to main diffraction planes: (100), (002), (101), (102), (110), (103), (200), (112)

and (201), in the hexagonal wurtzite structure. The peaks have been identified (JCPDS card no. 36-1451) by WinXPow software.

The FTIR spectra of sodium alginate (Fig. 2A) showed a broad peak at 3351 cm^{-1} for its hydrogen bonded OH group. Asymmetric and symmetric stretching of $-\text{COO}$ group of alginate was observed at 1638 and 1408 cm^{-1} , respectively (Kulkarni, Sreedhar, Mutalik, Setty, & Sa, 2010). In addition, sodium alginate showed a characteristic peak at 1022 cm^{-1} corresponding to C–O stretching vibration of its polysaccharide structure. The peak at 862 cm^{-1} corresponds to Na–O bond vibration (Samanta & Ray, 2014). Pure cellulose fibre showed characteristic peaks at around 3364 cm^{-1} , 2924 cm^{-1} and at around 1311 cm^{-1} corresponding to $-\text{OH}$ stretching frequency, $>\text{CH}_2$ stretching vibration and C–H bending mode respectively; characteristic bands at 1150 and 1015 cm^{-1} are assigned to the C–O–C from the glycosidic units or from β -(1,4)-glycosidic bonds (Raghavendra, Jayaramudu, Varaprasad, Ramesh, & Raju, 2014). The combination of the peaks corresponding to both sodium alginate and cellulose were observed in sodium alginate coated cellulose fibre. However, in case of cellulose-zinc oxide sodium alginate nanocomposite fibres, an additional peak distinctive for Zn–O–Zn vibrations was noticed at 533 cm^{-1} with slightly shift in the frequency of peaks corresponding to cellulose and sodium alginate (Ambika & Sundrarajan, 2015). This evidently indicates the composite bonding nature of nano ZnO with cellulose fibre through sodium alginate matrix.

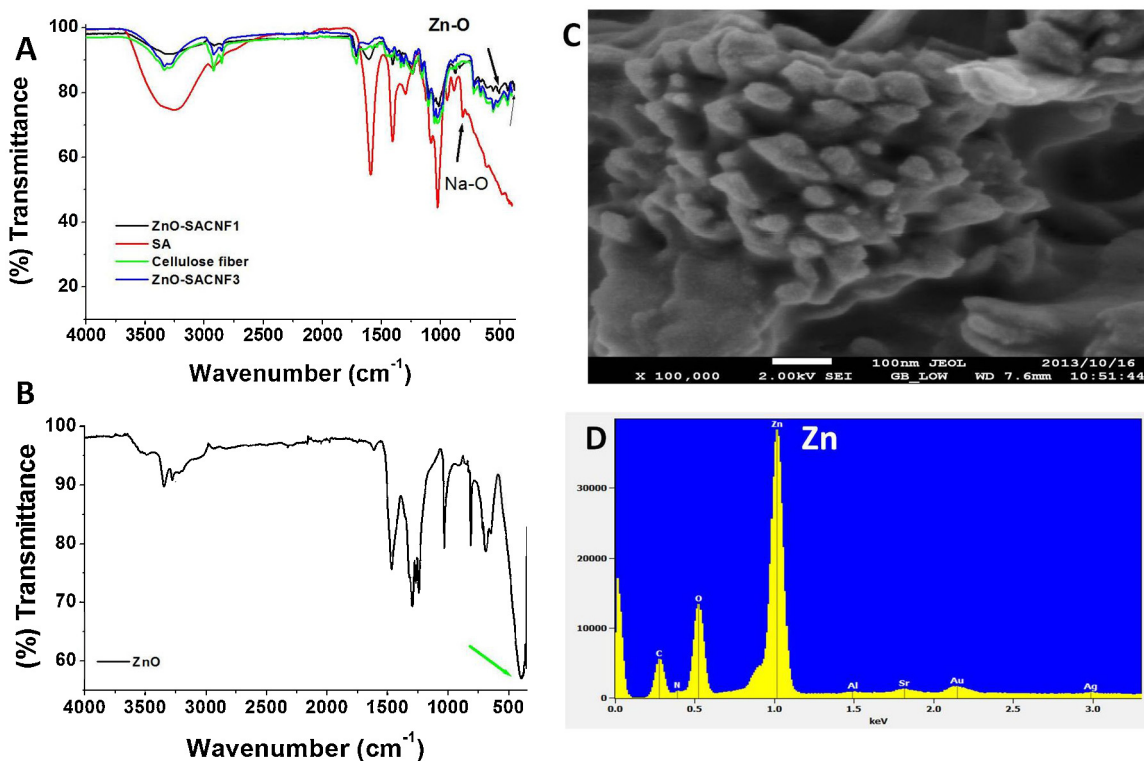


Fig. 2. FTIR spectra of (A) ZnO-SACNF1, SA, cellulose fibre, ZnO-SACNF3; (B) nano ZnO materials; (C) SEM images of ZnO and (D) EDS images of nano ZnO.

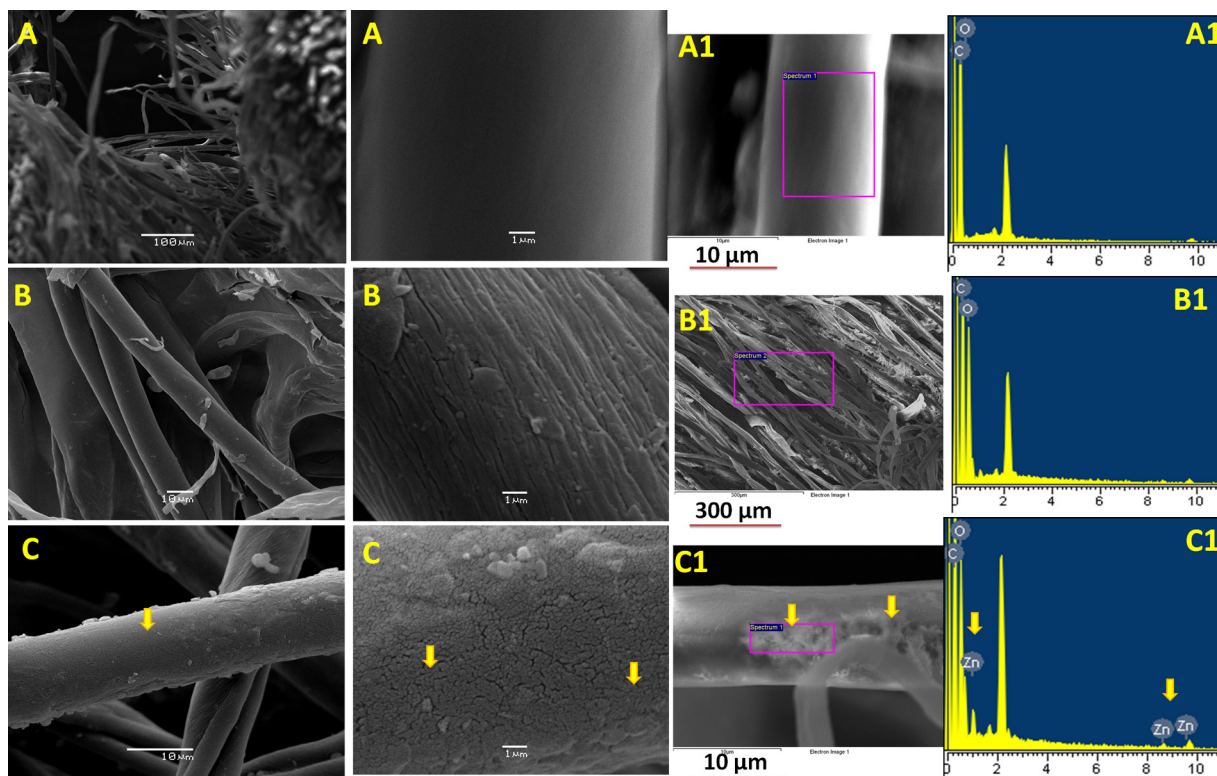


Fig. 3. SEM image of (A) cellulose fibre, (B) sodium alginate coated cellulose fibre, (C) ZnO-SACNF and EDS image of (A1) cellulose fibre, (B1) sodium alginate coated cellulose fibre, (C1) ZnO-SACNF.

The FTIR spectrum of zinc oxide (Fig. 2B) showed important peaks at 405 cm^{-1} and 697 cm^{-1} which indicate Zn–O stretching mode (Varaprasad, Ramam, Mohan Reddy, & Sadiku, 2014). The peaks were observed at $1600\text{--}1640$ and $3100\text{--}3600\text{ cm}^{-1}$ but not broad. This is due to the presence of traces of water after hydration by exposure of the ZnO in the open air (Morozov, Belousova, Ortega, Mafina, & Kuznetsov, 2015).

The detailed information on the morphology of the synthesized nano ZnO and ZnO–SACNF was revealed by SEM. The SEM image of the synthesized nano ZnO was presented in Fig. 2C. The image evidently showed the rod-like shape of zinc oxide nanoparticles with excellent alignment. The corresponding EDS analysis evidently confirmed the nano ZnO by giving characteristic peaks corresponding to mainly zinc and oxygen elements (Fig. 2D).

The presence of ZnO nanoparticles over the ZnO–SACNF were evident from the SEM images, which showed the distribution of nano ZnO (indicated with arrows) over the fibres (Fig. 3). However, the distribution pattern is absent in the case of pure cellulose fibre (Fig. 3A) and sodium alginate coated cellulose fibre (Fig. 3B). This indicates the distributed particles over ZnO–SACNF is nano ZnO. To confirm this prediction, SEM–EDS was carried out for pure cellulose fibre (Fig. 3A1), sodium alginate coated cellulose fibre (Fig. 3B1) and ZnO–SACNF fibre (Fig. 3C1). The data revealed that the peaks corresponding to elemental zinc and oxygen were showed only by ZnO–SACNF fibre but not by pure cellulose fibre and sodium alginate coated cellulose fibre (Fig. 3B2). Hence, the SEM–EDS strongly supported for the distribution of ZnO over cellulose fibres.

The thermal property of fibres is a valuable piece of evidence that provides the information on physical characteristics and the components present in the fibres as well. As shown in the TGA curves (Fig. 4), an initial weight loss at a temperature below $100\text{ }^{\circ}\text{C}$ was observed due to the loss of moisture present on the surface for all the samples. The primary thermogram of the synthesized ZnO nanoparticles showed the higher degradation between 224 and $314\text{ }^{\circ}\text{C}$ and a final residue of at $600\text{ }^{\circ}\text{C}$ (Fig. 4A) whereas the sodium alginate coated cellulose fibre (SACF) and ZnO–SACNF fibres showed the higher degradation at between $289\text{--}443\text{ }^{\circ}\text{C}$ and a final residue of at $600\text{ }^{\circ}\text{C}$ (Fig. 4B). The residual mass left over from the SACF (13%), ZnO–SACNF1 (15.25%) and ZnO–SACNF3 (17.75%), clearly indicates the existence of nano ZnO. Thermal studies led to the conclusion that with the increase in the percentage (%) of sodium alginate, the residual mass leftover also increases. This was due to rise in the number of nano ZnO over ZnO–SACNF with increase in sodium alginate concentration. The phenomenon is due to the overall rise in bonding interactions between ‘nano ZnO sodium alginate matrix’ and the polar groups of cellulose fibre that occurred with the increase in sodium alginate concentration. This raised the nano ZnO number effectively. In overall, TGA data demonstrates that ZnO–SACNF fibres are thermally more stable than the sodium alginate cellulose coated fibre.

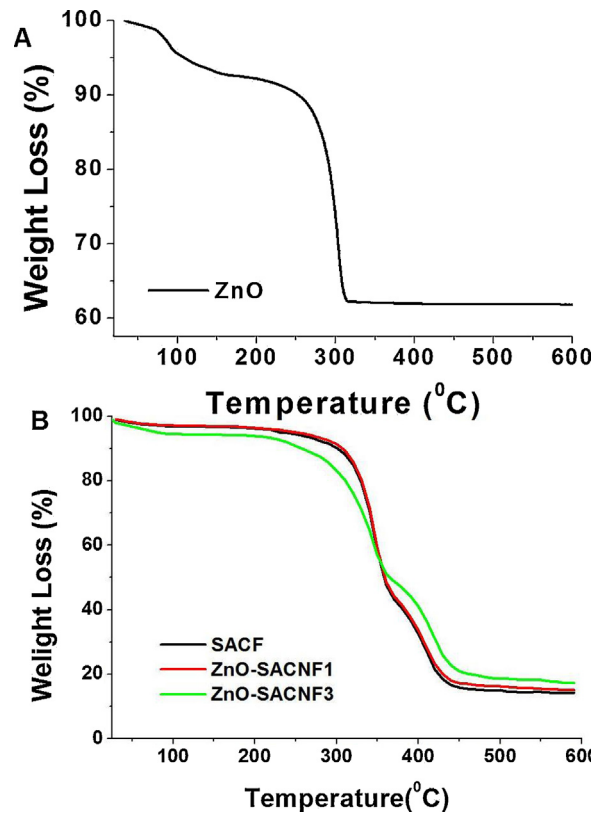


Fig. 4. TGA curves of (A) ZnO and (B) SACF, ZnO–SACNF1 and ZnO–SACNF3.

The tensile stress–strain curves data of sodium alginate coated cellulose fibres (SACFs) and ZnO–SACNF fibres were depicted in Table 1. The data illustrates the mechanical properties such as: maximum stress (Fig. 5A), Young’s modulus (Fig. 5B) and % elongation-at-break (Fig. 5C) of all the cellulose fibres. The results indicate that the ZnO–SACNF can be utilized for the longer duration of use without any significant damage or breakage.

4.1. Antibacterial activity

Destruction of bacteria is the key parameter that determines the utility of the developed fibres for various applications in bacteriaprone areas. The antimicrobial efficacy of the ZnO–SACNF fibres was tested against Gram-negative bacterium *E. coli*. The inhibition zone for all the fibres was found to be in between 2.1 and 3.6 mm, shown in Fig. 6. According to the Standard Antibacterial test “SNV 195920-1992”, specimens showing more than 1 mm microbial zone inhibition can be considered as good antibacterial agents (Pollini, Russo, Licciulli, Sannino, & Maffezzoli, 2009; Raghavendra et al., 2013, 2014). In the present investigation,

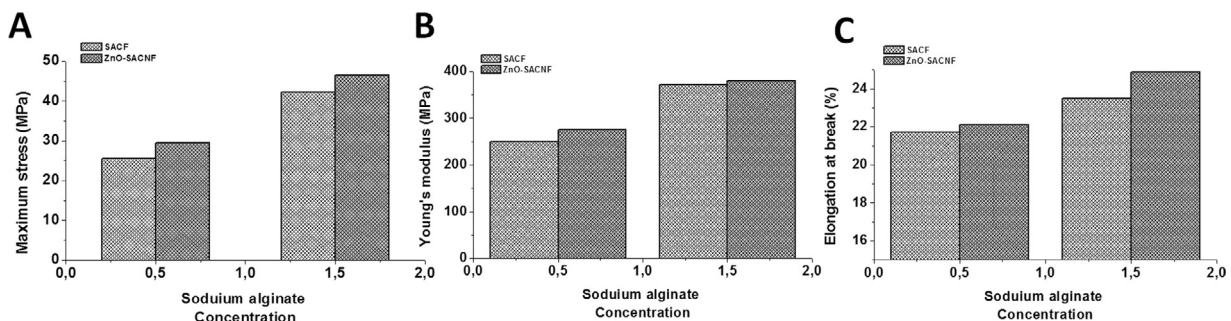


Fig. 5. Uniaxial stress–strain curves of SACF fibres and ZnO–SACNF fibres (A) maximum stress; (B) Young’s modulus; (C) elongation at break.

Table 1
Mechanical properties of the SACF and ZnO–SACNFs.

Sample code	Maximum stress (Mpa)	Young modulus (MPa)	Elongation at break (%)
SACF (0.5% SA)	22.5	250	21.7
ZnO–SACNF (0.5% SA)	29.5	275	22.1
SACF (1.5% SA)	42.2	372	23.5
ZnO–SACNF (1.5% SA)	46.5	379	24.9

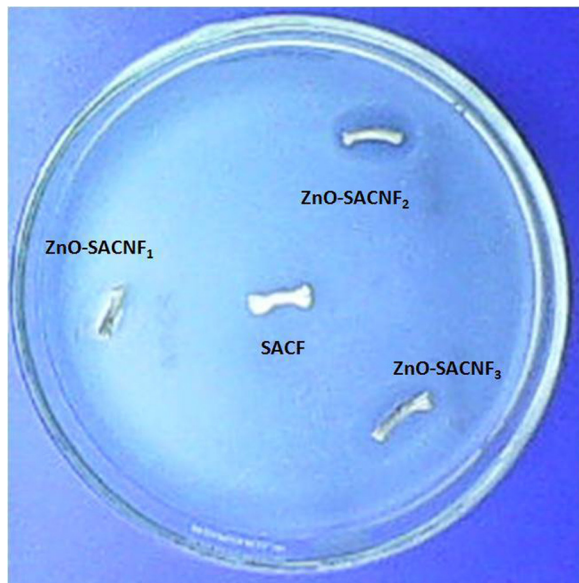


Fig. 6. Antibacterial activity of SACF, ZnO–SACNF₁, ZnO–SACNF₂ and ZnO–SACNF₃.

the inhibition zones exhibited by cellulose fibre, ZnO–SACNF₁, ZnO–SACNF₂ and ZnO–SACNF₃ against *E. coli* were 0.0, 2.1, 3.2, and 3.6 mm, respectively. Hence, the developed ZnO–SACNF from the current approach can be considered as good antibacterial agents and effective in killing the microbes. Further, it can be noticed that when pure cellulose fibre showed no inhibition zone, the fabricated fibres showed the inhibition zones of the order: ZnO–SACNF₁ < ZnO–SACNF₂ < ZnO–SACNF₃. This order is quite expected and seemed to be in accordance with the amount of nano ZnO present in ZnO–SACNF fibres. It was concluded from the TGA analysis that the nano ZnO content proceeding increases with the increase of SA. Hence, the observed inhibition zones were also exhibited the similar trend and proved the results were in proportional with the nano ZnO content. The particular mechanism of the antimicrobial activity of ZnO is still a matter of dispute. Some researchers consider that it might be a consequence of the generation of hydrogen peroxide (H₂O₂) on its surface (Trandafilović et al., 2012).

5. Conclusion

Various zinc oxide–sodium alginate–cellulose nanocomposite fibres (ZnO–SACNF) were successfully fabricated by a simple and cost-effective procedure. The possible zinc oxide nanoparticles were synthesized by precipitation method. The synthesized zinc oxide nanoparticles possess rods-like shape alignment with an interplanar d-spacing of 0.246 nm corresponding to the (101) planes of hexagonal wurtzite structure acquiring an average particle size 25 ± 5 nm. The successfully fabricated ZnO–SACNF showed excellent antibacterial activity against *E. coli*. Hence, from the viewpoint of biomedical applications, the fabricated ZnO–SACNF fibres may be utilized as antibacterial fabrics for wound dressing applications in the bacterial prone zone.

Acknowledgements

The author Kokkarachedu Varaprasad wishes to acknowledge the PAI Proyecto No. 781302011, CONICYT, Chile and the CIPA, CONICYT Regional, and GORE BIO BIO R08C1002.

References

- Ambika, S., & Sundrarajan, M. (2015). Antibacterial behaviour of Vitex negundo extract assisted ZnO nanoparticles against pathogenic bacteria. *Journal of Photochemistry and Photobiology B: Biology*, 146, 52–57.
- Gardner, D. J., Oporto, G. S., Mills, R., & Samir, M. A. S. A. (2008). Adhesion and surface issues in cellulose and nanocellulose. *Journal of Adhesion Science and Technology*, 22(5–6), 545–567.
- Gunalan, S., Sivaraj, R., & Rajendran, V. (2012). Green synthesized ZnO nanoparticles against bacterial and fungal pathogens. *Progress in Natural Science: Materials International*, 22(6), 693–700.
- Jayaramudu, T., Raghavendra, G. M., Varaprasad, K., Sadiku, R., & Raju, K. M. (2013). Development of novel biodegradable Au nanocomposite hydrogels based on wheat: For inactivation of bacteria. *Carbohydrate Polymers*, 92(2), 2193–2200.
- Jayaramudu, T., Raghavendra, G. M., Varaprasad, K., Sadiku, R., Ramam, K., & Raju, K. M. (2013). Iota–Carrageenan-based biodegradable AgO nanocomposite hydrogels for the inactivation of bacteria. *Carbohydrate Polymers*, 95(1), 188–194.
- Kolya, H., Pal, S., Pandey, A., & Tripathy, T. (2015). Preparation of gold nanoparticles by a novel biodegradable graft copolymer sodium alginate-g-poly (N,N-dimethylacrylamide-co-acrylic acid) with anti micro bacterial application. *European Polymer Journal*, 66(0), 139–148.
- Kulkarni, R. V., Sreedhar, V., Mutalik, S., Setty, C. M., & Sa, B. (2010). Interpenetrating network hydrogel membranes of sodium alginate and poly(vinyl alcohol) for controlled release of prazosin hydrochloride through skin. *International Journal of Biological Macromolecules*, 47(4), 520–527.
- Morozov, I. G., Belousova, O. V., Ortega, D., Mafina, M. K., & Kuznetsov, M. V. (2015). Structural, optical, XPS and magnetic properties of Zn particles capped by ZnO nanoparticles. *Journal of Alloys and Compounds*, 633(0), 237–245.
- Mucha, H., Hoter, D., & Swerev, M. (2002). Antimicrobial finishes and modifications. *Melliand International*, 8, 148–151.
- Nagender Reddy, P., Eladia Maria, P. M., & Josef, H. (2009). Gold and nano-gold in medicine: Overview, toxicology and perspectives. *Journal of Applied Biomedicine*, 7(2), 75–91.
- Pollini, M., Russo, M., Licciulli, A., Sannino, A., & Maffezzoli, A. (2009). Characterization of antibacterial silver coated yarns. *Journal of Materials Science: Materials in Medicine*, 20(11), 2361–2366.
- Raghavendra, G. M., Jayaramudu, T., Varaprasad, K., Mohan Reddy, G. S., & Raju, K. M. (2015). Antibacterial nanocomposite hydrogels for superior biomedical applications: A facile eco-friendly approach. *RSC Advances*, 5(19), 14351–14358.
- Raghavendra, G. M., Jayaramudu, T., Varaprasad, K., Ramesh, S., & Raju, K. M. (2014). Microbial resistant nanocurcumin–gelatin–cellulose fibers for advanced medical applications. *RSC Advances*, 4(7), 3494–3501.
- Raghavendra, G. M., Jayaramudu, T., Varaprasad, K., Sadiku, R., Ray, S. S., & Mohana Raju, K. (2013). Cellulose–polymer–Ag nanocomposite fibers for antibacterial fabrics/skin scaffolds. *Carbohydrate Polymers*, 93(2), 553–560.
- Raghavendra, G. M., Varaprasad, K., & Jayaramudu, T. (2015). Chapter 2 – Biomaterials: Design development and biomedical applications. In S. T. G. Ninan (Ed.), *Nanotechnology applications for tissue engineering* (pp. 21–44). Oxford: William Andrew Publishing.
- Samanta, H. S., & Ray, S. K. (2014). Synthesis, characterization, swelling and drug release behavior of semi-interpenetrating network hydrogels of sodium alginate and polyacrylamide. *Carbohydrate Polymers*, 99, 666–678.
- Shalumon, K. T., Anulekha, K. H., Nair, S. V., Nair, S. V., Chennazhi, K. P., & Jayakumar, R. (2011). Sodium alginate/poly(vinyl alcohol)/nano ZnO composite nanofibers for antibacterial wound dressings. *International Journal of Biological Macromolecules*, 49(3), 247–254.
- Trandafilović, L. V., Božanić, D. K., Dimitrijević-Branković, S., Luyt, A. S., & Djoković, V. (2012). Fabrication and antibacterial properties of ZnO–alginate nanocomposites. *Carbohydrate Polymers*, 88(1), 263–269.
- Vaideki, K., Jayakumar, S., Rajendran, R., & Thilagavathi, G. (2008). Investigation on the effect of RF air plasma and neem leaf extract treatment on the surface modification and antimicrobial activity of cotton fabric. *Applied Surface Science*, 254(8), 2472–2478.

Varaprasad, K., Ramam, K., Mohan Reddy, G. S., & Sadiku, R. (2014). Development and characterization of nano-multifunctional materials for advanced applications. *RSC Advances*, 4(104), 60363–60370.

Varaprasad, K., Vimala, K., Raghavendra, G. M., Jayaramudu, T., Sadiku, E. R., & Ramam, K. (2015). Chapter 10 – Cell encapsulation in polymeric

self-assembled hydrogels. In S. T. G. Ninan (Ed.), *Nanotechnology applications for tissue engineering* (pp. 149–171). Oxford: William Andrew Publishing.

Zhao, J., Zhang, W., An, X., Liu, Z., Xie, E., Yang, C., et al. (2014). Room-temperature ferromagnetism in ZnO nanoparticles by electrospinning. *Nanoscience and Nanotechnology Letters*, 6(5), 446–449.